

Electron Mobility Maximum in near Critical Argon Gas¹

A.F.Borghesani^{2,3} and M.Santini²

¹ Paper presented at the Fourteenth Symposium on Thermophysical Properties, June 25-30, 2000, Boulder, Colorado, U.S.A.

² Istituto Nazionale per la Fisica della Materia, Dipartimento di Fisica “G. Galilei”, University of Padua, Via F.Marzolo, 8, I-35131 Padua, Italy

³ To whom correspondence should be addressed.

ABSTRACT

We report measurements of drift mobility μ of excess electrons in dense Argon gas in proximity of the critical point of the liquid–vapor transition. We investigated the density and electric field dependence of μ at two temperatures fairly close to the critical one, namely $T = 162.30$ K ($T/T_c \approx 1.08$) and $T = 152.15$ K ($T/T_c \approx 1.01$) ($T_c = 150.7$ K) in a density range ($0.5 \leq N \leq 14$) atoms·nm³ ($0.06 \leq N/N_c \leq 1.73$), encompassing the critical region of Ar ($N_c = 8.08$ atoms·nm⁻³). At the lowest temperature we observed a maximum of the zero–field density–normalized mobility $\mu_0 N$ at the same density where it was observed in the liquid. We show that a density–modified kinetic model describes well all features of μ in the gas phase even at densities comparable to those of the liquid. We therefore argue that the electron scattering processes in the liquid phase could be described in terms of kinetic theory rather than in terms of the usual deformation potential model.

KEY WORDS: excess electrons, drift mobility, multiple scattering effects, kinetic theory, deformation potential theory.

1. INTRODUCTION

The investigation of the transport properties of excess electrons in dense non-polar gases provides the opportunity to study the effect of the environment on the electron-atom interaction in a disordered system. Close to the critical point the gas density can be largely varied with a reasonable change of pressure, so we can shed light on the nature and dynamics of the states of excess electrons in dense fluids and on how they evolve from the dilute gas regime, where the kinetic theory is valid, towards the liquid regime.

An important quantity is the electron mobility μ defined as the ratio between the mean velocity v_D acquired by an electron drifting in a medium under the action of an externally applied and uniform electric field and the field strength E : $\mu = v_D/E$. The kinetic theory, valid for dilute gases, predicts that the zero-field mobility μ_0 (defined as $\mu_0 = \lim_{E \rightarrow 0} \mu$) is related to the e -atom scattering cross section for momentum transfer σ_{mt} by

$$\mu_0 N = \frac{4e}{3(2\pi m)^{1/2} (k_B T)^{5/2}} \int_0^\infty \frac{\epsilon}{\sigma_{mt}(\epsilon)} e^{-\epsilon/k_B T} d\epsilon \quad (1)$$

where m and e are the electron mass and charge, respectively, ϵ is the electron energy, N is the gas density, and k_B is the Boltzmann constant [1].

For a given cross section, Eq. (1) predicts that the zero-field density-normalized mobility $\mu_0 N$ is independent of N . However, large deviations from this prediction, called *anomalous density effects*, are experimentally observed even in the simplest systems such as the noble gases [2]. In He [3] and Ne [4], where the e -atom interaction is dominated by short-range repulsive forces, there is a *negative density effect*, i.e., $\mu_0 N$ decreases with increasing N , eventually leading to the formation of localized electron states at high enough densities and in the liquid.

In Ar, on the contrary, where the long-range polarization interaction is very strong, there is a *positive density effect* because $\mu_0 N$ increases with N [5]. Moreover, in liquid Ar and liquified heavier noble gases, the mobility is comparable to that in

the crystalline state [6]. This behavior is commonly attributed to the existence of a conduction band in the liquid. Therefore, it is interesting to investigate the transition from the classical single scattering picture in the dilute gas to multiple scattering at higher densities and the eventual formation of extended or localized electron states in the liquid.

In order to explain the *anomalous density effects* several theories have been developed in the past. They all are based on the realization that at high densities the average interatomic distance becomes comparable to the deBroglie wavelength λ of the electron. Therefore, the classical picture of scattering breaks down and quantum effects become important. Moreover, also the mean free path ℓ becomes comparable to λ and multiple scattering effects come into play [2].

Although the physical situation seems clear, nonetheless the two density effects were explained in terms of different mechanisms. For the negative one it was assumed that there is an increase of the electron scattering rate with increasing N because the electron mean free path is becoming comparable to its wavelength. The electron wavepacket is multiply scattered off several scattering centers and undergoes a quantum self-interference process that reduces its mobility. At particularly high densities this process eventually leads to the formation of a mobility edge and to localized electron states [7].

For the positive effect, on the contrary, a complex and density-dependent quantum shift of the ground state energy of the excess electrons in the dense medium is taken into account. This shift increases the average energy of the electron and, owing to the energy dependence of the atomic cross section, decreases the scattering rate [8].

However, recent and accurate mobility measurements in Ne [4, 9] and Ar [10, 11] and their analysis have led to an unified description of the scattering of excess electrons off atoms of noble gases at high densities. A heuristic model, known as the BSL model, has been developed, which incorporates the most relevant *multiple*

scattering effects into the *single scattering picture* of kinetic theory [10].

Three main multiple scattering effects can be singled out, whose net effect is to dress the atomic cross section producing a density-dependent effective cross section. The first one is a density-dependent shift $V_0(N)$ of the ground-state energy of an excess electron in the medium. According to the SJC model $V_0(N)$ consists of two contributions [12]

$$V_0(N) = U_P(N) + E_k(N) \quad (2)$$

U_P is a negative potential energy term arising from the screened polarization interaction of the electron with the gas atoms. E_k is a positive kinetic energy contribution due to excluded volume effects (and, hence, it increases with N) and is obtained by imposing on the electron ground-state wavefunction the conditions of average translational symmetry about the equivalent Wigner-Seitz (WS) cell centered about each atom. V_0 may be either > 0 (as for He [13] and Ne) or < 0 (as for Ar [14, 15]), depending on the relative size of U_P and E_k , but only the positive kinetic contribution E_k must be added to the electron kinetic energy when the scattering properties (e.g., the scattering cross sections) have to be evaluated. In other words, the electron energy distribution function is shifted to higher energies by the amount E_k [9].

The second effect is an enhancement of the electron scattering rate due to quantum self-interference of the electron wavefunction scattered off atoms along paths connected by time-reversal symmetry [16]. This effect is intimately related to the *weak localization* regime of the electronic conduction in disordered solids and to the Anderson localization transition [17]. It depends on the ratio of the electron wavelength to its mean free path $\lambda/\ell = N\sigma_{mt}\lambda$. In the case of Ar, $N\sigma_{mt}\lambda < 1$ and the effect can be treated within the linearized AI model [18], where the momentum transfer cross section is enhanced by the factor $1 + N\sigma_{mt}\lambda/\pi$.

Finally, the third multiple scattering effect arises from correlations among scatterers. The electron wavepacket spans over a region containing several atoms and is scattered off all of them simultaneously. The partial scattering amplitudes must be

summed coherently in order to get the total scattered wavepacket and the net result is that the cross section must be suitably weighted by the static structure factor of the fluid which is related to the gas compressibility [19].

In our modified kinetic model (or, BSL model) the density-normalized mobility μN is calculated according to the following equations [10]

$$\mu N = - \left(\frac{e}{3}\right) \left(\frac{2}{m}\right)^{1/2} \int_0^\infty \frac{\epsilon}{\sigma_{mt}^* (\epsilon + E_k)} \frac{dg}{d\epsilon} d\epsilon \quad (3)$$

$g(\epsilon)$ is the Davydov–Pidduck electron energy distribution function given by [20, 21]

$$g(\epsilon) = A \exp \left\{ - \int_0^\infty \left[k_B T + \frac{M}{6mz} \left(\frac{eE}{N\sigma_{mt}^*} \right)^2 \right]^{-1} dz \right\} \quad (4)$$

M is the Ar atomic mass. g is normalized as $\int_0^\infty z^{1/2} g(z) dz = 1$.

The effective momentum transfer scattering cross section is

$$\sigma_{mt}^*(w) = \mathcal{F}(w) \sigma_{mt}(w) \left[1 + \frac{2\hbar N \mathcal{F}(w) \sigma_{mt}(w)}{(2mw)^{1/2}} \right] \quad (5)$$

Here $w = \epsilon + E_k(N)$ is the electron energy shifted by the kinetic zero-energy contribution E_k . It is the group velocity $v = [2(w - E_k)/m]^{1/2}$ which contributes to the energy equipartition value arising from the gas temperature [21]. The factor \mathcal{F} is the Lekner factor [19] that accounts for the correlations among scatterers

$$\mathcal{F}(k) = \frac{1}{4k^4} \int_0^{2k} q^3 S(q) dq \quad (6)$$

with $k^2 = 2m\epsilon/\hbar^2$. The static structure factor $S(q)$ in the near-critical region has the form [22]

$$S(q) = \frac{S(0) + (qL)^2}{1 + (qL)^2} \quad (7)$$

where $S(0)$ is related to the gas isothermal compressibility χ_T by the relation

$$S(0) = Nk_B T \chi_T \quad (8)$$

The correlation length L is defined by

$$L^2 = 0.1l^2 [S(0) - 1] \quad (9)$$

where $l \approx 10 \text{ \AA}$ is the so-called *short-range correlation length* [22].

From the experiments with Ne [4, 9] and Ar [10] (here, at $T = 162.7 \text{ K}$ up to $N/N_c \approx 0.88$) we found that the kinetic energy shift can be quite accurately calculated according to the WS model as $E_k = E_{WS} \equiv \hbar^2 k_0^2 / 2m$, where k_0 is obtained by solving the eigenvalue equation

$$\tan [k_0 (r_s - \tilde{a}(k_0))] - k_0 r_s = 0 \quad (10)$$

$r_s = (3/4\pi N)^{1/3}$ is the radius of the WS cell and \tilde{a} is the hard-core radius of the Hartree-Fock potential for rare gas atoms. In our model, according to a suggestion found in literature [12], we have estimated \tilde{a} from the total scattering cross section as $\tilde{a} = \sqrt{\sigma_T/4\pi}$.

The BSL model is in excellent agreement with data in Ar gas also at $T = 152.5 \text{ K}$ and up to $N \approx 10 \text{ atoms} \cdot \text{nm}^3$, provided that one realizes that the WS model is inappropriate for very high N and that E_k must be deduced from the experiment [11]. Obviously, the question arises if the BSL model has been pushed beyond its limits of applicability or if different physical mechanisms set in for momentum transfer processes at such large N . Indeed, in liquid Ar a maximum of the mobility of thermal electrons has been observed at the density where V_0 is minimum [23]. This mobility maximum has been interpreted in terms of the deformation potential theory as due to electrons scattering off long-wavelength collective modes of the fluid which modulate the bottom V_0 of the conduction band. The spatial inhomogeneity of the electron ground-state energy is the source of scattering. This *phononic* model [23, 24] predicts the existence of the mobility maximum in Ar at the correct value $N \approx 12.5 \text{ atoms} \cdot \text{nm}^3$, but it fails to predict the density- and the electric field dependence of μN as the BSL model does. For these reasons, we have extended the mobility measurements in Ar gas at $T = 152.15 \text{ K}$ up to $N \approx 14 \text{ atoms} \cdot \text{nm}^3$ in order to ascertain if the mobility maximum is a feature typical of the liquid only or if it can be observed also in the gas phase. In this case there could be strong reasons to extend the kinetic picture of scattering even to the liquid [25].

2. EXPERIMENT

We used the same pulsed photoinjection technique already employed for electron and O_2^- ion mobility measurements in dense noble gases Ne [9, 26], He [27, 28], and Ar [29]. We refer to literature for details. We recall here only the main features of the apparatus. The measuring cell is mounted in a triple-shield cryostat and is thermoregulated within ± 0.01 K. The temperature is measured with a calibrated Pt resistor. The cell withstands pressures up to 10 MPa. The gas pressure P is measured with an uncertainty of ± 1 kPa. The gas density N is calculated from T and P by using a recent and accurate equation of state [30]. We used Argon gas with a nominal impurity content, mainly Oxygen, of ≈ 1 p.p.m. The impurity level is reduced to a fraction of a p.p.b. by recirculating the gas through a purification circuit consisting of an activated-charcoal cold trap and an Oxisorb purifier cartridge. Electrons are photoinjected into the gap between two parallel-plate electrodes and drift under the influence of an externally applied electric field. During the drift motion they induce a current in the external circuit. The current is integrated by means of a passive RC circuit in order to improve the signal-to-noise ratio. The electron drift time τ is measured by analyzing the signal waveform [31]. The mobility is calculated from t as $\mu = d^2/\tau V$, where d is the electrode spacing and V is the applied voltage. The estimated uncertainty on μ is $\approx 5\%$.

3. RESULTS AND DISCUSSION

Measurements were taken at $T = 162.30$ K and $T = 152.15$ K. In Fig. 1 we show sample μN data as a function of the reduced electric field E/N at $T = 152.15$ K. For small E/N μN levels off at the zero-field value $\mu_0 N$ pertaining to thermal electrons. At small and medium densities μN shows the maximum due to the Ramsauer-Townsend (RT) minimum of the cross section [32] for $E/N = (E/N)_{max} \approx 4 \times 10^{-24}$ V cm². Then, for large E/N the curves for all densities collapse onto a single curve well described by the kinetic equations [1] in combination with the measured

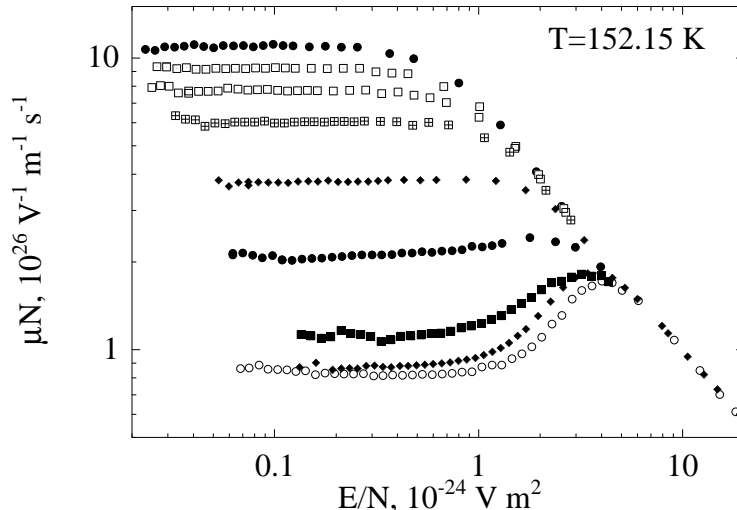


Figure 1: μN as a function of E/N for $T = 152.15$ K. The densities are (from top) $N = 10.40, 10.16, 9.935, 9.352, 8.048, 6.708, 6.146, 3.117, 1.097$ atoms \cdot nm $^{-3}$.

cross sections [32]. In the frame of the BSL model this behavior is clearly understood. At small energies (hence, at low fields) the extension of the wavepacket, as measured by its wavelength $\lambda = h/\sqrt{2m\epsilon}$, is pretty large. As the average electron energy is increased by increasing E/N , the wavepacket shrinks and the effects of multiple scattering decrease. Therefore, the experimental points for large E/N must converge to the prediction of the classical kinetic theory.

The coordinate of the mobility maximum $(E/N)_{max}$ decreases with increasing N until the maximum itself disappears for $N \geq N_c$, as shown in Fig. 2. Also this behavior is quite easily understood. At $(E/N)_{max}$ the average electron energy equals the energy of the RT minimum of the cross section $\langle\epsilon\rangle = \epsilon_{RT}$. Since $\langle\epsilon\rangle = (3/2)k_B T + E_k(N) + f(E/N)$, where $f(E/N)$ is a monotonically increasing function of E/N [1], and since E_k increases with N , $(E/N)_{max}$ must decrease in order to keep $\langle\epsilon\rangle = \epsilon_{RT}$ constant when N increases. Finally, for even larger N the electron energy distribution function is so shifted by E_k as to sample the cross section at $\epsilon > \epsilon_{RT}$

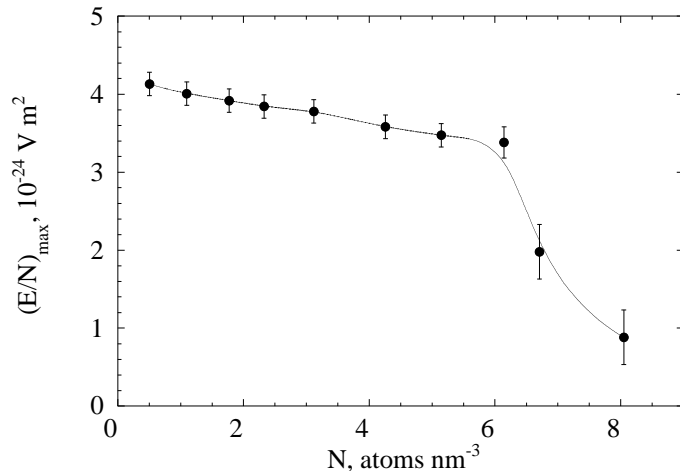


Figure 2: Decrease of $(E/N)_{max}$ with increasing N for $T = 152.15$ K. The line is a guide for the eye.

and the mobility maximum as a function of E/N disappears.

In Fig. 3 we show the zero-field density-normalized mobility $\mu_0 N$ as a function of N for $T = 162.3$ K and $T = 152.15$ K. Also previous data at $T = 162.7$ K [10] are shown for comparison. Two are the most important features shown by data in Fig. 3. The first one is that, for small to medium N , $\mu_0 N$ increases with N for both temperatures. Again, this fact is easily explained by the BSL model. At $E/N \rightarrow 0$ electrons do not practically gain energy from the electric field and therefore their average energy is $\langle \epsilon \rangle \ll \epsilon_{RT}$. In this region σ_{mt} decreases rapidly with increasing energy [32]. Since $\mu_0 N$ is a sort of weighted average of the inverse cross section, as expressed by Eq. (1), to a first approximation it can be calculated by evaluating $1/\sigma_{mt}$ at the average energy. So, $\mu_0 N$ can increase with N only if $\langle \epsilon \rangle$ increases with N , owing to the shape of the cross section. This fact strongly supports the conclusion that there is a density-dependent shift of the electron kinetic energy and that this shift is positive and increases with density.

The second most important feature is the existence, for $T = 152.15$ K, of a maximum of $\mu_0 N$ at $N = N_m \approx 12.5 \text{ atoms} \cdot \text{nm}^{-3}$, at nearly the same density as

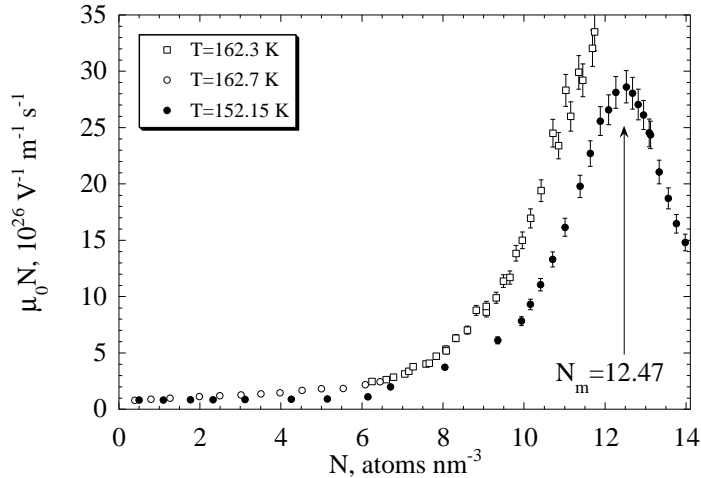


Figure 3: $\mu_0 N$ as a function of the density for $T = 162.5, 162.3,$ and 152.15 K.

observed in the liquid. The presence of this $\mu_0 N$ maximum for $N = N_m$ also in the dense gas raises the question if there is a change in the physical mechanisms determining the electron transport properties as N increases beyond a certain threshold. At low and medium N the single scatterer approximation is valid and electrons can be described as scattered off individual atoms though the scattering properties must be modified so as to include multiple scattering effects. As N increases electrons might be scattered off collective excitations of the fluid. However, there are several reasons to extend the kinetic picture rather than to adopt the different point of view of the deformation potential models. First of all, a gas, even at such high N , does not support phonons. Then, the *phononic* models do not agree very well with the experiment [14, 24] and, moreover, they do not allow the calculation of the very important E/N -dependence of μN because they are developed only for thermal electrons.

We have therefore implemented the BSL model for such high N . We have determined $E_k(N)$ by fitting Eq. (3)–(7) with $E/N = 0$ to the experimental $\mu_0 N$ data. We used literature data for the cross sections [32]. In Fig. 4 we show the values of $E_k(N)$ obtained in this way and compare them with the prediction of the WS model

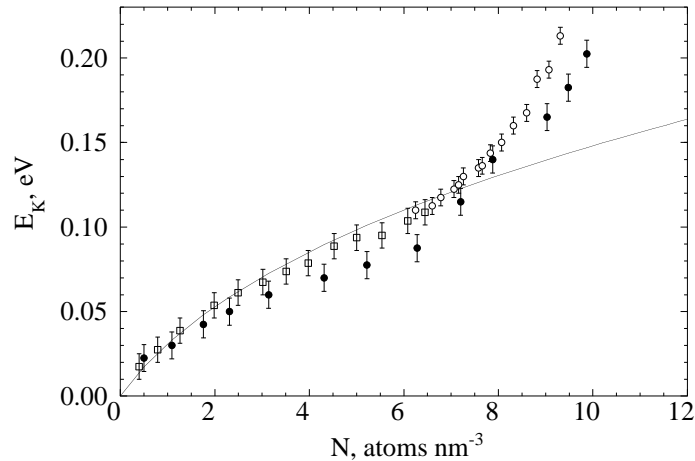


Figure 4: E_k as a function of N . Open squares: $T = 162.7$ K [10], open circles: $T = 162.3$ K, closed points: $T = 152.15$ K. The line is Eq. (10).

Eq. (10). Also previous results for $T = 162.7$ K are shown for comparison [10]. Beside the small differences obtained for the two different temperatures, which may be attributed to the larger compressibility for the temperature closer to T_c , the experimentally determined values of E_k agree quite well with the prediction of the WS model up to $N \approx 7$ atoms \cdot nm $^{-3}$, as already pointed out in the previous experiment on Ar [10]. For larger N E_k increases faster with N than in the WS model. This is not surprising because it is known that the WS model is applicable only when $r_s \gg \tilde{a}$. If we relax the condition that the WS model is valid up to very high N and use the E_k values determined experimentally from $\mu_0 N$, the BSL model reproduces accurately the experimental data up to $N \approx 10$ atoms \cdot nm $^{-3}$. In this density range the BSL model shows a very good degree of internal consistency because the full E/N -dependence of μN is well reproduced by using the value of E_k determined by fitting the model to the zero-field data, as shown in Fig. 5 by the dotted lines. At small and medium N the position and strength of the mobility maximum as a function of the reduced electric field is reproduced quite accurately as well as its disappearing when N increases. This also confirms the hypothesis that the density-

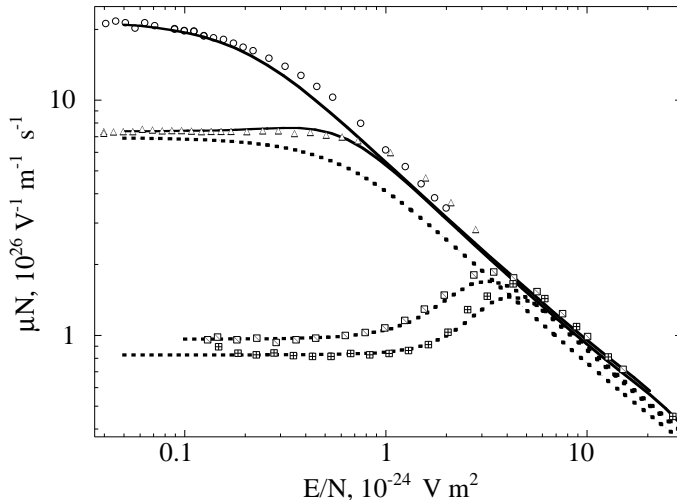


Figure 5: μN as a function of E/N for $T = 152.15$ K. From top: $N = 13.33, 9.935, 5.144, 0.502$ atoms \cdot nm 3 . Dotted lines: prediction of the BSL. Solid lines: calculations with σ_{eff} .

dependent kinetic energy shift E_k is so large as to shift the average electron energy to values $\geq \epsilon_{RT}$.

In this form, however, the model does not reproduce the $\mu_0 N$ maximum for $N = N_m \approx 12.5$ atoms \cdot nm 3 , although the overall behavior can be traced back to the density-dependent quantum shift of the electron energy distribution function and on the shape of the cross section. On one hand, the scattering cross sections are known with limited accuracy as far as the strength and position of the RT minimum are concerned. Different choices of σ_{mt} give different strength and position values of the $\mu_0 N$ maximum [11]. On the other hand, the use of an effective scattering cross section may give excellent agreement with the data, as pointed out in literature [11, 25]. The E/N -dependence of μN and the N -dependence of $\mu_0 N$ at very high N can be accurately described if the effective cross section σ_{mt}^* of Eq. (5) is scaled by a density dependent factor $c(N)$ of order unity. $c(N)$ is an adjustable parameter but is independent of E/N and of the electron energy. It has therefore no influence on the E/N -dependence of μN . When introducing $c(N)$ the energy shift $E_k(N)$ is no longer considered as an empirical parameter, but it is rather set equal to the WS

value E_{WS} given by Eq. (10). By substituting σ_{mt}^* in Eq. (3) by $\sigma_{eff} = c(N)\sigma_{mt}^*$, with $c = \mathcal{O}(1)$, the E/N -dependence of μN is reproduced very well as shown by the solid lines in Fig. 5.

The shape of the effective cross section σ_{eff} at thermal energy is shown in Fig. 6 as a function of the electron energy. Also the atomic momentum transfer cross section [32] is shown for a comparison. In order to plot $\sigma_{eff}(N) = c(N)\sigma_{mt}^*(\epsilon = (3/2)k_B T + E_{ws})$ and $\sigma_{mt}(\epsilon)$ on the same scale the density has been converted to energy by means of the WS model Eq. (10).

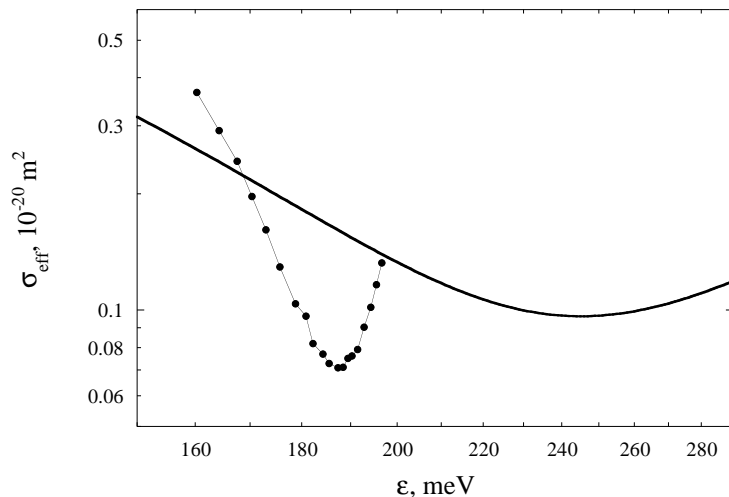


Figure 6: Comparison between σ_{eff} (dots) and σ_{mt} [32] (solid line). N has been converted to ϵ by means of Eq. (10).

It is remarkable the similarity of σ_{eff} to the e -atom cross section of Ar. Similarly to its atomic companion, σ_{eff} has a minimum surely related to the RT minimum of σ_{mt} . Also the strength of σ_{eff} is close to that of σ_{mt} , although the minimum occurs at lower energies and is narrower. This is probably due to the use of Eq. (10) for the $N \rightarrow \epsilon$ conversion. As one can see from Fig. 4, E_{ws} is smaller than the experimentally determined E_k . The use of the experimental E_k instead of E_{ws} would broaden the minimum of σ_{eff} and shift it to larger energies.

In any case, taking into account the limited accuracy of the atomic cross section, the use of an approximated form $\mathcal{F}(\epsilon)$ of an energy-dependent structure function,

the neglect of a density dependence of the electron mass, i.e., an effective mass, and the neglect of the influence of density fluctuations on the distribution function, the results are very encouraging. They give firm basis to the attempts of using the kinetic theory even in the liquids [25] although these results claim for more refined theoretical models.

REFERENCES

1. L.G.Huxley and R.W.Crompton, *The Diffusion and Drift of Electrons in Gases*, (Wiley, New York , 1974).
2. A.F.Borghesani and M.Santini, in *Linking the Gaseous and Condensed Phases of Matter. The behavior of Slow Electrons*, NATO ASI Series **B 326**, L.G.Christophorou, E.Illenberger, and W.F.Schmidt eds. (Plenum, New York, 1994), p.259.
3. J.L.Levine and T.M.Sanders, *Phys. Rev.* **154**:138 (1967).
4. A.F.Borghesani and M.Santini. *Phys. Rev.* **A 42**:7377 (1990).
5. A.K.Bartels, *Phys. Lett* **44A**:403 (1973).
6. J.A.Jahnke, L.Meyer, and S.A.Rice, *Phys. Rev.* **A 3**:734 (1971).
7. A.Y.Polishuk, *Physica* **124 C**:91 (1984).
8. T.F.O'Malley, *J. Phys.* **B 13**:1491 (1980).
9. A.F.Borghesani, L.Bruschi, M.Santini, and G.Torzo, *Phys. Rev.* **A 37**: 4828 (1988).
10. A.F.Borghesani, M.Santini, and P.Lamp, *Phys. Rev.* **A 46**: 7902 (1992).
11. P.Lamp and G.Buschhorn, *Phys. Rev.* **B 50**: 16824 (1994).
12. B.E.Springett, J.Jortner, and M.H.Cohen, *J. Chem. Phys.* **48**:2720 (1968).

13. J.R.Broomall, W.D.Johnson, and D.G.Onn, *Phys. Rev.* **B 14**:2819 (1976).
14. R.Reininger, U.Asaf, I.T.Steinberger, and S.Basak, *Phys. Rev.* **B 28**:4426 (1983).
15. A.F.Borghesani, G.Carugno, and M.Santini, *IEEE Trans.* **EI-26**:615 (1991).
16. G.Ascarelli, *Phys. Rev.* **B 33**:5825 (1986).
17. P.W.Adams, D.A.Browne, and M.A.Paalanen, *Phys. Rev.* **B 45**:8837 (1992).
18. V.M.Atrazhev and I.T.Iakubov, *J. Phys.* **D 10**:2155 (1977).
19. J.Lekner, *Philos. Mag.* **18**:1281 (1968).
20. M.H.Cohen and J.Lekner, *Phys. Rev.* **158**:305 (1967).
21. G.H.Wannier, *Statistical Physics* (Dover, New York, 1966).
22. J.E.Thomas and P.W.Schmidt, *J. Chem. Phys.* **39**:2506 (1963).
23. S.Basak and M.H.Cohen, *Phys. Rev.* **B20**:3404 (1979).
24. Y.Naveh and B.Laikthman, *Phys. Rev.* **B 47**:3566 (1993).
25. K.Kaneko, Y.Usami, and K.Kitahara, *J. Chem. Phys.* **89**:6420 (1988).
26. A.F.Borghesani, D.Neri, and M.Santini, *Phys. Rev.* **E 48**: 1379 (1992).
27. A.F.Borghesani, D.Neri, and M.Santini, *Phys. Rev.* **E 56**: 2137 (1997).
28. A.F.Borghesani, F.Chiminello, D.Neri, and M.Santini, *Int. J. Thermophys.* **16**: 1235 (1995).
29. A.F.Borghesani, D. Neri, and A. Barbarotto, *Chem. Phys. Lett.* **267**: 116 (1997).
30. C.Tegeler, R.Span, and W.Wagner, *VDI Fortschritt-Berichte* **3**, Nr. 480, (VDI Verlag, Düsseldorf, 1997).

31. A.F.Borghesani and M.Santini, *Meas. Sci. Technol.* **1**:939 (1990).
32. M.Weyhreter, B.Barzick, A.Mann, and F.Linder, *Z. Phys.* **D 7**:333 (1988).